750027

An Examination of the Performance of Spark Ignition Engines Using Hydrogen-Supplemented Fuels

J. F. Stocky, M. W. Dowdy, and T. G. Vanderbrug
California Institute of Technology

SINCE 1973 THE JET PROPULSION LABORATORY has been engaged in experiments using hydrogen to supplement gasoline and thus permit operation of a spark-ignited internal combustion engine at conditions leaner than those which would support the combustion of gasoline alone. Such operation resulted in reduced combustion temperatures with attendant lower NO_x emissions and improved engine thermal efficiency. Results of work using a hydrogen/gasoline fuel system have been published (1)*. Such an approach, however, is not new. As early as 1927, hydrogen/gasoline mixtures were tested by the Zeppelin Co. in airship engines with a view toward improving the range of dirigibles. (2)

The difficulties of storage and distribution have rendered pure hydrogen impractical as a near-term fuel. Consequently, the work at JPL has focused on the partial oxidation of gasoline to provide a hydrogen-rich gas with which to supplement the gasoline/air mixture flowing to the engine. An on-board hydrogen generator in which this partial oxidation reaction would take place was described in Ref. 3 and the results of early tests with a 350 CID Chevrolet V-8 engine and a hydrogen generator were described in Ref. 4.

This paper presents the results of an analytical investigation of the hydrogen-supplemented fuels system undertaken as part of an Environmental Protection Agency evaluation of this system. This evaluation also included experimental data taken with a 350 CID Chevrolet engine operating with a hydrogen generator. The experimental configuration was described in Ref. 4.

The analytical models described in this paper were three-fold:

(1) A model of the hydrogen generator subsystem and its associated auxiliaries such as an air compressor and heat exchanger.

(2) A semiempirical model of the engine operating on hydrogen generator products.

(3) A simulation of the Federal Driving Cycle using the characteristics of a 1973 Chevrolet Impala vehicle and the predicted performance of the engine/generator combination.

This paper presents the results of one phase of research carried out at the Jet Propulsion Laboratory, California Institute of Technology, sponsored by the National Aeronautics and Space Administration, under Contract No. NAS 7-100, and by the Environmental Protection Agency.

* Numbers in parentheses designate References at end of paper.

ABSTRACT

The performance of a hydrogen-supplemented fuels system is predicted using a semiempirical model. The prediction of this model is compared to data obtained during engine dynamometer tests of a hydrogen generator/multicylinder engine system. The test data and the predictions are also compared to the fuel consumption and emissions of the same engine in its stock configuration and indicate that the hydrogen-supplemented fuels system can improve BSFC 10-15% and simultaneously reduce NO_x emissions to a level consistent with the 1977 EPA standard. The performance of an optimized hydrogen generator/engine system is estimated. With these comparisons and estimates used as a basis, the potential of the hydrogen-supplemented fuels system is identified.

These analytical tools then permitted a prediction of fuel economy and NO_x emissions over the Federal Driving Cycle to be made. Changes in the performance of elements of the total system could then be related to changes in the predicted driving cycle performance.

Comparison of the predictions of these analytical models with engine and chassis dynamometer data indicated good agreement among them. The engine/hydrogen generator system performance was then predicted assuming an improved engine ability to operate at a lean condition and an increased compression ratio. These predictions indicated that mileage over the Federal Driving Cycle could be improved by as much as 25% relative to the 1973 baseline vehicle and NO_x emissions simultaneously reduced to 0.2 gm/mile.

SUBSYSTEM AND SYSTEM DESCRIPTION

The overall lean operation of the hydrogen-supplemented fuels system was achieved by adding a hydrogen-rich gas to the engine gasoline/air mixture. This hydrogen would permit lean operation yielding increased engine efficiency and reduced NO_x emissions. For these analyses, a hydrogen generator subsystem comprised of the hydrogen generator, its heat exchangers, and its gasoline and air supplies was defined. A block diagram is shown in Fig. 1.

The system was comprised of the engine and this hydrogen generator subsystem, which imposed additional loads on it. These loads were a function of hydrogen generator flow rate and resulted from the following elements of the subsystem:

(1) The air compressor and its drive mechanism.

(2) The fuel pump.

(3) The additional water pump loads for the coolant heat exchanger.

(4) The pressure drop of the components in the air and product flow streams.

These loads were aggregated and the "nominal" auxiliary load curve shown in Fig. 2 was calculated. To obtain a best and worst case estimate of these loads, the component performance estimates were multiplied by the factors presented in Table 1; the "minimum" and "maximum" auxiliary load curves shown in Fig. 2 were then obtained.

HYDROGEN GENERATOR – The hydrogen generator employed partial oxidation of a rich gasoline/air mixture in the presence of a catalyst to provide a hydrogen-rich product gas. The Girdler catalyst used in this application consisted of nickel deposited on alumina pellets. Its operation is described in Ref. 3. The product gas composition used in these analyses is shown in Table 2.

AIR COMPRESSOR – Air is supplied to the hydrogen generator by a variable-speed compressor. Heat exchange with the hydrogen generator product gas is used to preheat this air to 500°F. After mixing with vaporized gasoline the mixture is introduced into the hydrogen generator and reacted on the surface of the catalyst. The assumed air compressor efficiency is shown in Fig. 3. (5)

Fig. 1 - Hydrogen-supplemented fuels system

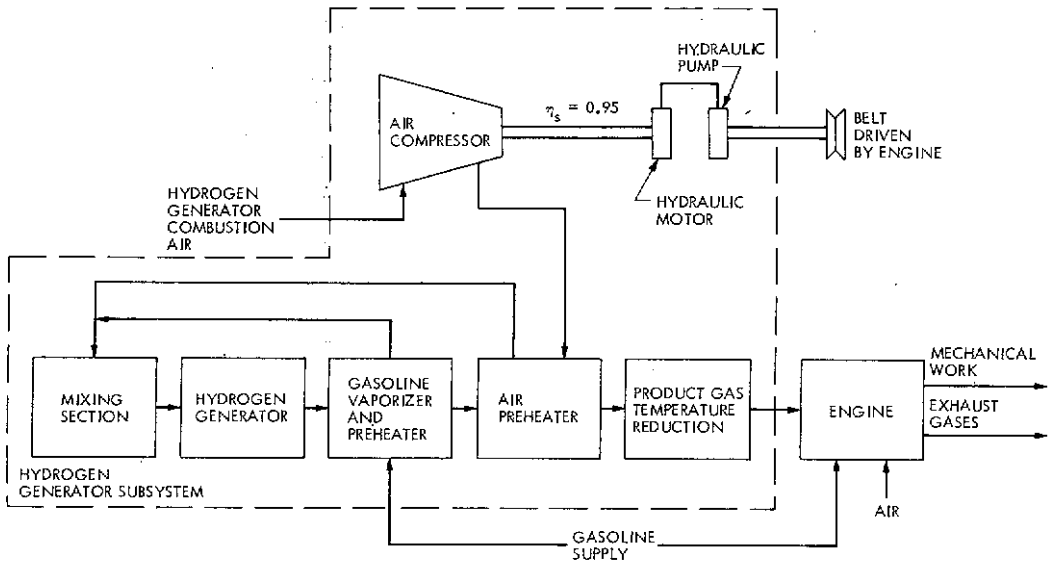

A hydraulic pump/motor combination was assumed for the air compressor drive. Though more complex than any production-type system would be, this permitted air compressor speed to be decoupled from engine speed. The resulting ease of analysis made its use in the model attractive. In addition, the loads such a system would impose on the engine would be known to be conservative.

Table 1. Range of Component Parameter Variation

Parameter	Performance Penalty Factors * Minimum	Nominal	Maximum
Air compressor efficiency (η_c)	1.10	1.0	0.8
Hydraulic motor efficiency (η_m)	1.10	1.0	0.9
Hydraulic pump efficiency (η_p)	1.10	1.0	0.9
Pressure loss factors $K = \Delta_p/q_c$	0.9	1.0	1.20
Generator HX effectiveness (ϵ)	1.0	1.0	1.0

*Multiplication factor to penalize system: "best" system performance

$$\eta_{c,\ max} = \eta_{c,\ nom} \times \text{factor (min)}$$

"worst" system performance

$$\eta_{c,\ min} = \eta_{c,\ nom} \times \text{factor (min)}$$

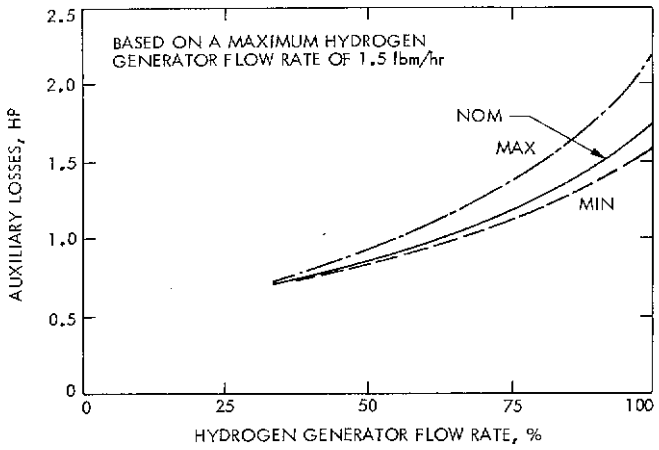

Fig. 2 - Auxiliary load curve for hydrogen generator subsystem

Table 2. Hydrogen Generator Average Output Composition

Component	Volume %
H_2	21.22
CH_4	1.11
CO	23.24
CO_2	1.05
H_2O	1.33
N_2	52.05
	100.00

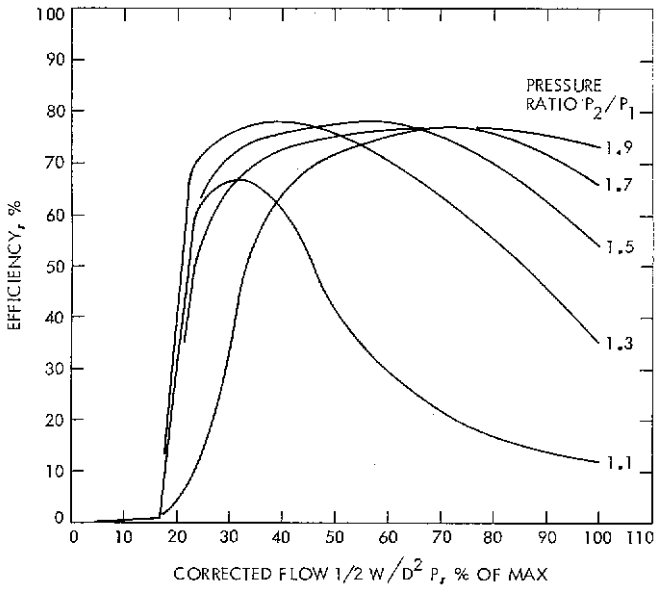

Fig. 3 - Air compressor performance

The hydraulic pump performance is shown in Fig. 4 (6). The hydraulic motor efficiency was taken to be 0.875 of the hydraulic pump efficiency, and the efficiency of the coupling between the pump, the motor, and the compressor was taken to be 0.95.

HEAT EXCHANGERS: FUEL AND AIR – The fuel heat exchanger is used to vaporize and heat the hydrogen generator gasoline before it is mixed with the reaction air. The reaction air is also heated to a temperature which will prevent condensation of the fuel during the mixing process.

The effectiveness required of these heat exchangers is presented in Fig. 5. The relatively low values of the required effectiveness indicated that high heat exchanger performance was not required for this application.

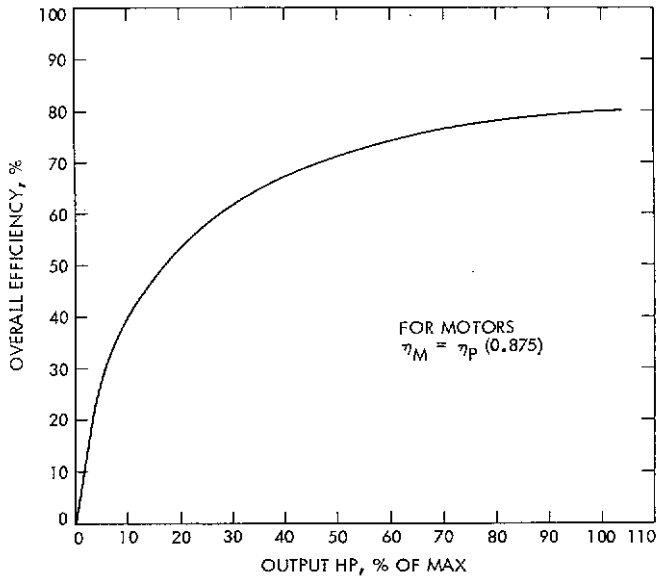

Fig. 4 - Hydraulic pump performance

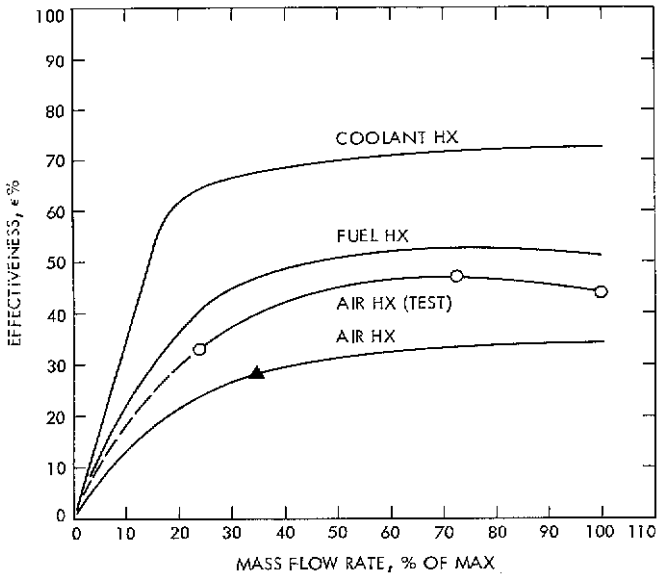

Fig. 5 - Required heat exchanger effectiveness

HEAT EXCHANGER: COOLANT – To preclude autoignition it was decided to hold the temperature of the hydrogen generator product gas at or below 525°F when it was introduced at the engine induction system. However, this product gas, even after heat exchange with the input fuel and air, was still too warm to be mixed immediately with the engine gasoline/air mixture. Reducing this temperature was accomplished in the analysis by rejecting heat to the engine coolant system.

DESCRIPTION OF CALCULATION SCHEME

In this section the calculations of system efficiency and NO_X emissions as a function of hydrogen generator flow rate and of engine gasoline and air flow rates are described. These will then be integrated with the model of the hydrogen generator subsystem to estimate system brake specific fuel consumption and NO_X emissions as a function of brake mean effective pressure (BMEP) and engine speed (rpm). A simulation of the Federal Driving Cycle was then used with these estimates to predict the system fuel consumption and emissions when driven over that cycle.

The calculation of system efficiency and of NO_X emissions is most easily visualized by introducing two dimensionless variables. One is the ratio of the gasoline flow rate to the engine divided by the flow rate of gasoline to the hydrogen generator

$$\psi = \frac{\dot{m}_{gE}}{\dot{m}_{gG}}$$

The other is the effective equivalence ratio ϕ'_E: that is engine equivalence ratio ϕ_E modified to account for the flow rate of noncombustibles in the hydrogen generator product gas:

$$\phi'_E = \frac{\begin{array}{l}\text{stoichiometric air flow for engine gasoline flow rate}\end{array}}{\begin{array}{l}\text{actual air flow rate}\end{array}} \quad \frac{\begin{array}{l}\text{stoichiometric air flow for hydrogen generator product flow rate}\end{array}}{\begin{array}{l}\text{flow rate of non-combustibles in hydrogen generator product gas}\end{array}}$$

This effective equivalence ratio is used to compensate, approximately, for the reduction in combustion temperature caused by this diluent flow rate. The composition of the hydrogen generator product gas used in these analyses is shown in Table 2. This composition is the average over the flow rate range of that provided by the hydrogen generator described in Ref. 3 when operating at a generator equivalence ratio ϕ_G of 2.75. The molecular weight of the noncombustibles in this flow was estimated to be 28.1, and their specific heat C_P was calculated to be 0.26 Btu/lbm/°F.

SYSTEM THERMAL EFFICIENCY – System indicated thermal efficiency η_{IS} was calculated from ψ, ϕ'_E, and the hydrogen generator product gas composition. The ratio θ_G of the heat of combustion of the hydrogen generator product gas to the heat of combustion of the gasoline used to make that product gas is

$$\theta_G = \frac{\dot{m}_H h_H + \dot{m}_{CO} h_{CO} + \dot{m}_{CH4} h_{CH4}}{\dot{m}_{gG} h_g}$$

where $\dot{m}_i$ is the mass flow rate of the ith component, h_i is the lower heating value of the ith component, and subscripts H, CO, CH4, g, G refer to hydrogen, carbon monoxide, methane, gasoline, and hydrogen generator respectively.

At an operating point of the system determined by ψ and ϕ'_E, the indicated thermal efficiency η_{IS} can be calculated as

$$\eta_{IS} = \eta_{IE} \frac{\theta_G + \psi}{1 + \psi}$$

The engine indicated thermal efficiency was assumed in these analyses to be a function of ϕ'_E only. The assumed functional relationship was

$$\eta_{IE} = 0.50 - 0.17\,\phi'_E$$

This relationship is shown in Fig. 6 and compared to data more fully described in Ref. (8). The data is reasonably well represented by this relationship until, as ever leaner operation of the engine is attempted, increasing flame speed causes engine efficiency to begin to decrease.

OPERATING CONSTRAINTS – The range of ψ and ϕ'_E over which the engine can operate is limited by two operating constraints: a wide open throttle volume flow rate constraint and a lean operating constraint.

At wide open throttle (WOT) the maximum volume flow which can pass through the engine is a function of

the engine volumetric efficiency e_v, the engine speed N, and the engine displacement V_D. Neglecting the volume displaced by the gasoline flowing to the engine, the sum of the volume flow rates of engine air and hydrogen generator products must equal this engine volume flow rate. This constraint can be plotted as a function of ψ and ϕ'_E as shown in Fig. 7, typical of that for various engine speeds and hydrogen generator flow rates.

The expression used to obtain these constraints is derived in the Appendix. The WOT engine volumetric efficiency was assumed to be constant, with a value of 0.7. The engine displacement assumed for all calculations was 350 CID.

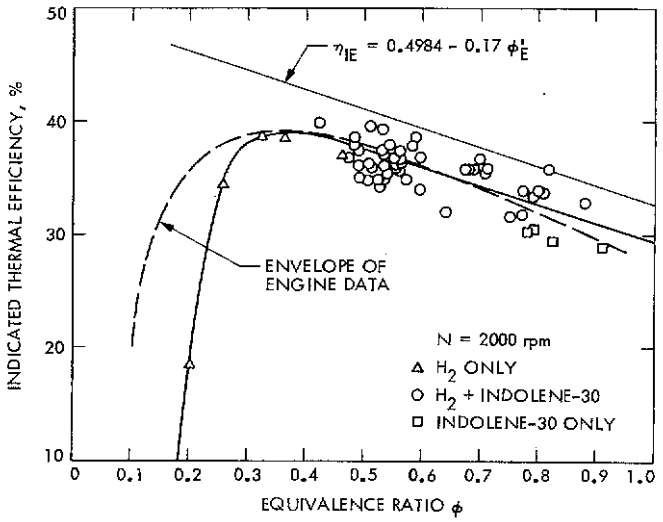

Fig. 6 - Indicated thermal efficiency for V-8 engine

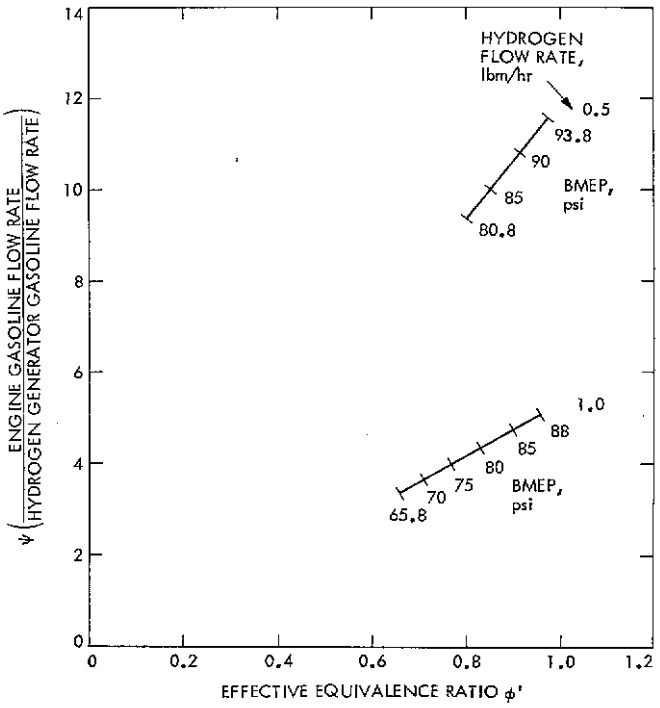

Fig. 7 - Wide open throttle operating constraints

The engine lean limit constraint was estimated in two ways. First, Bureau of Mines data (7) was used to estimate the lean flammability limit of mixtures of hydrogen generator products and gasoline according to Le Chatelier's rule. The results of this calculation are shown in Fig. 8 as the curve labeled "calculated lean limit." The system indicated thermal efficiency for operation on this lean limit was calculated and is shown in Fig. 9.

Second, the results of V-8 engine/hydrogen generator tests on an engine dynamometer were used to

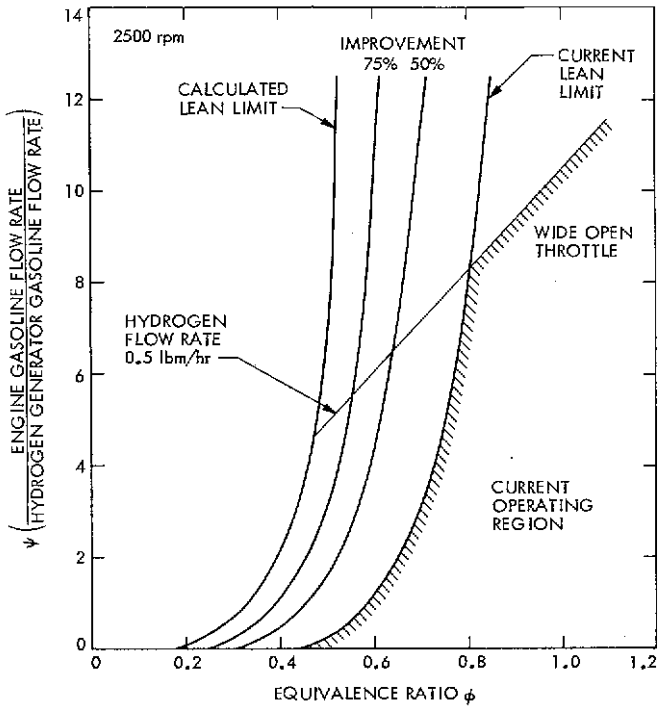

Fig. 8 - Lean limit constraint for engine/hydrogen generator system

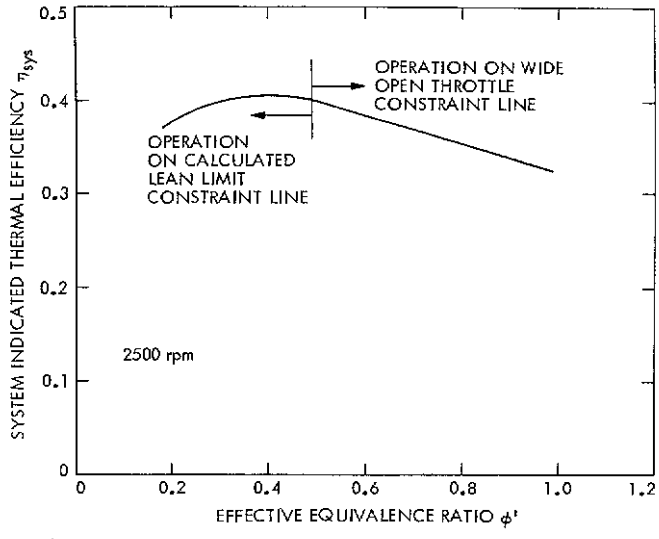

Fig. 9 - System indicated thermal efficiency

define empirically the locus of engine maximum efficiency points. These are shown on Fig. 8 as "current lean limit."

These curves then represent a constraint in that an operating point to the left or right of them is achieved at the expense of the system efficiency. The region in Fig. 8 to the right (richer) of the WOT constraint line and the current lean limit represents the operating region presently available. For any value of ψ, efficiency is maximized by operating as lean as these two constraints will permit.

OUTPUT POWER – At any operating point within this operating region, output power can be calculated once throttle setting, hydrogen generator flow rate, ψ, and ϕ_E' have been specified. The assumed functional relationship for engine thermal efficiency allows engine efficiency to be calculated once ϕ_E' has been specified. Hydrogen generator flowrate, specified herein in terms of the flow rate of the hydrogen contained in the product gas, and ψ taken together provide the flow rate of gasoline to the engine. Thus the total heat of combustion flowing to the engine is known, and with the indicated engine efficiency yields the engine indicated output power.

The engine friction horsepower (FHP) was calculated from a power series in rpm which was fit to data provided by General Motors, as shown in Fig. 10.

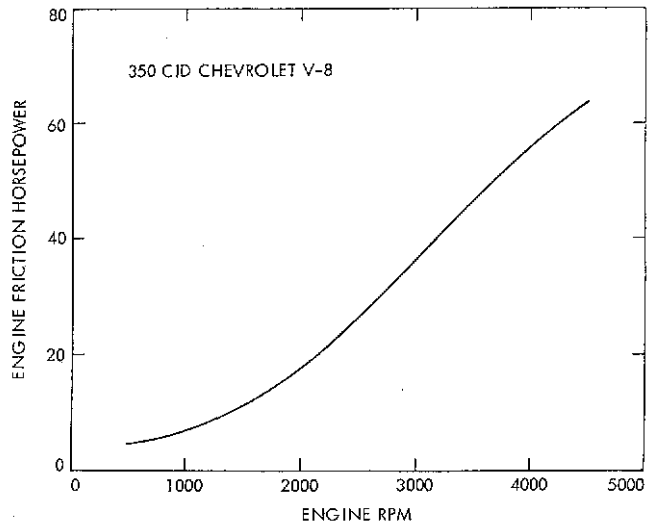

Fig. 10 - Engine friction horsepower characteristic

The horsepower required by the hydrogen generator subsystem was calculated as a function of hydrogen generator flow rate according to the relationship shown in Fig. 2. The friction horsepower and the power required by the hydrogen generator subsystem were subtracted from the engine indicated power to obtain engine brake power output.

EMISSIONS CALCULATION – The system model assumed that indicated specific NO_x ($ISNO_x$) emissions were a function of effective equivalence ratio and hydrogen generator flow rate, as shown in Fig. 11. These curves were the result of fitting data taken for three hydrogen generator flow rates over a broad range of engine loads and speeds (8). Linear interpolation was used to obtain $ISNO_x$ values as a function of hydrogen generator flow rate.

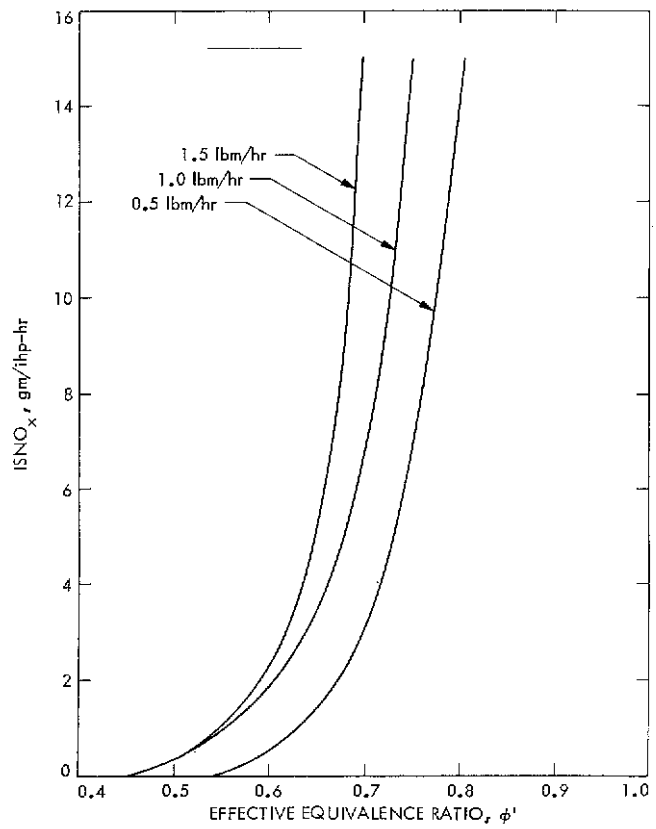

Fig. 11 - $ISNO_x$ versus effective equivalence ratio

CASES CONSIDERED – This model was used to predict system brake specific fuel consumption (BSFC) and brake specific NO_x ($BSNO_x$) emissions as a function of engine brake mean effective pressure (BMEP) and engine speed (rpm). Two hydrogen generator flow rates were considered, those providing 0.5 lbm/hr and 1.0 lbm/hr of hydrogen in the product gas. In addition, a variable hydrogen generator flow rate case was considered.

The variable hydrogen generator flow rate case can be visualized by referring to Fig. 12, wherein the wide open throttle constraints for 2500 rpm are shown for hydrogen generator flow rates providing 0.5 lbm/hr and 1.0 lbm/hr of hydrogen. Maximum engine output power was obtained by operating along the 0.5 lbm/hr WOT constraint between an equivalence ratio of 1.0 and the lean limit constraint. WOT operation down the lean limit constraint was continued by increasing hydrogen generator flow rate and decreasing the flow rate of gasoline to the engine. The maximum hydrogen generator flow rate considered was that providing 1.0 lbm/hr hydrogen. Once this maximum hydrogen generator flow rate was reached, throttling was used to reduce engine output. Over the throttling range of the hydrogen generator, gasoline flow to the engine and the hydrogen generator flow rate were maintained

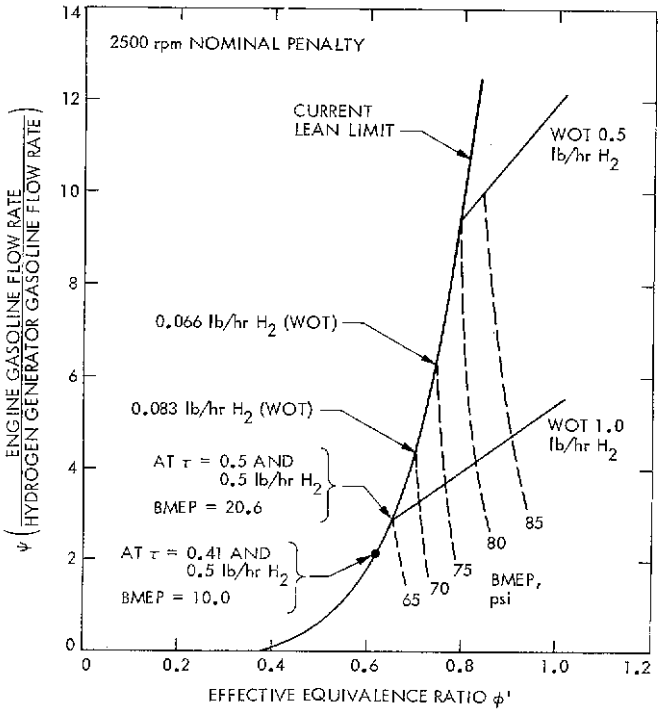

Fig. 12 - Variable flow rate hydrogen generator system operation

proportional to the air flow. Thus, operation over this range of hydrogen generator flow rate and air throttling occurred at constant ψ and ϕ_E^I. Once the minimum hydrogen generator flow rate, 0.5 lbm/hr hydrogen flow, had been reached, output was further reduced by additional throttling of air and engine gasoline at constant hydrogen generator flow such that operation on the lean limit constraint was maintained. When only hydrogen generator products flowed to the engine, $\psi = 0$, no further reductions in engine output could be obtained. Also shown on Fig. 12 are the WOT brake mean effective pressure (BMEP) output of the engine and the BMEP's corresponding to reduced throttle operation.

Thus, engine operation with three hydrogen flow rate conditions was examined:

(1) Constant hydrogen generator flow rate providing 0.5 lbm/hr of hydrogen.

(2) Constant hydrogen generator flow rate providing 1.0 lbm/hr of hydrogen.

(3) Variable hydrogen generator flow rate between those flow rates providing 0.5 and 1.0 lbm/hr of hydrogen according to the strategy outlined above.

The losses due to auxiliary loads in the hydrogen generator subsystem were also treated parametrically. In addition to the "nominal" load associated with this subsystem as a function of hydrogen generator flow rate, a "maximum" and a "minimum" load were used. These were used both to assess the sensitivity of system performance to the accuracy of these estimates and to provide an upper and lower bound to system performance.

In addition to these three cases, a case with no hydrogen generator subsystem losses charged to the engine was examined. This case permitted direct comparison with test data taken under equivalent conditions.

Several different engine configurations were examined. The baseline configuration consisted of the hydrogen generator subsystem and the 350 CID Chevrolet V-8 engine with 8.5:1 compression ratio operating with the lean limit constraint labeled "current lean limit." System performance was examined for two cases with improved lean limit: one lean limit constraint which was moved half-way toward the calculated constraint from the current constraint labeled "50% improved lean limit"; another which was moved three-fourths this distance and labeled "75% improved lean limit" (see Fig. 8).

The effect of compression ratio was evaluated by calculating system performance with an assumed compression ratio of 10:1. The effect of compression ratio on NO_x emission and system efficiency was estimated using the model described in Ref. 9.

COMPARISON WITH DATA – To obtain an estimate of the agreement between the BSFC and $BSNO_x$ predictions of the model and the values measured in testing, the model was used to predict these data for each of the BMEP/rpm points at which data was obtained for both the hydrogen generator flow rates. These flow rates were those providing 0.5 lbm/hr and 1.0 lbm/hr hydrogen in the hydrogen generator product gas. The system configuration consisted of

(1) A 350 CID Chevrolet V-8 engine with an 8.5:1 compression ratio operating at the current lean limit.

(2) A hydrogen generator, none of whose auxiliary requirements were supplied by the engine, corresponding to the no-penalty case.

For the 0.5 lbm/hr hydrogen flow case, a total of 24 data points were compared. These points covered the engine speed range from 1000 to 3000 rpm with BMEP between 9.3 and 83.2 psi. Over this range, predicted BSFC on the average was within 1.2% (rms: root mean square) of the measured value. Predicted $BSNO_x$ on the average was within 25% (rms) of the measured value. (8)

For the 1.0 lbm/hr hydrogen flow case a total of 21 data points were compared. These points covered the engine speed range from 1000 to 3000 rpm, with BMEP between 9.5 psi and 87.5 psi. Over this range, predicted BSFC on the average was within 1.6% (rms) of the measured value, and predicted $BSNO_x$ was within 25% (rms) of the measured value. (8) It was noted during this comparison that the predicted NO_x emission tended to be higher than those measured.

The output of this model was then used to provide the input information necessary to draw contours of BSFC and $BSNO_x$ in the BMEP/RPM plane. To illustrate their general nature, one of each of the BSFC and $BSNO_x$ contour plots are shown in Figs. 13 and 14. The case for which these contours were drawn was:

Variable hydrogen generator flow rate.

50% improved lean limit.

8.5:1 compression ratio.

SIMULATION OF THE FEDERAL DRIVING CYCLE – To provide an estimate of the fuel consumption and NO_x emissions which would result if a hydrogen generator/engine system with the characteristics predicted by the model were driven over

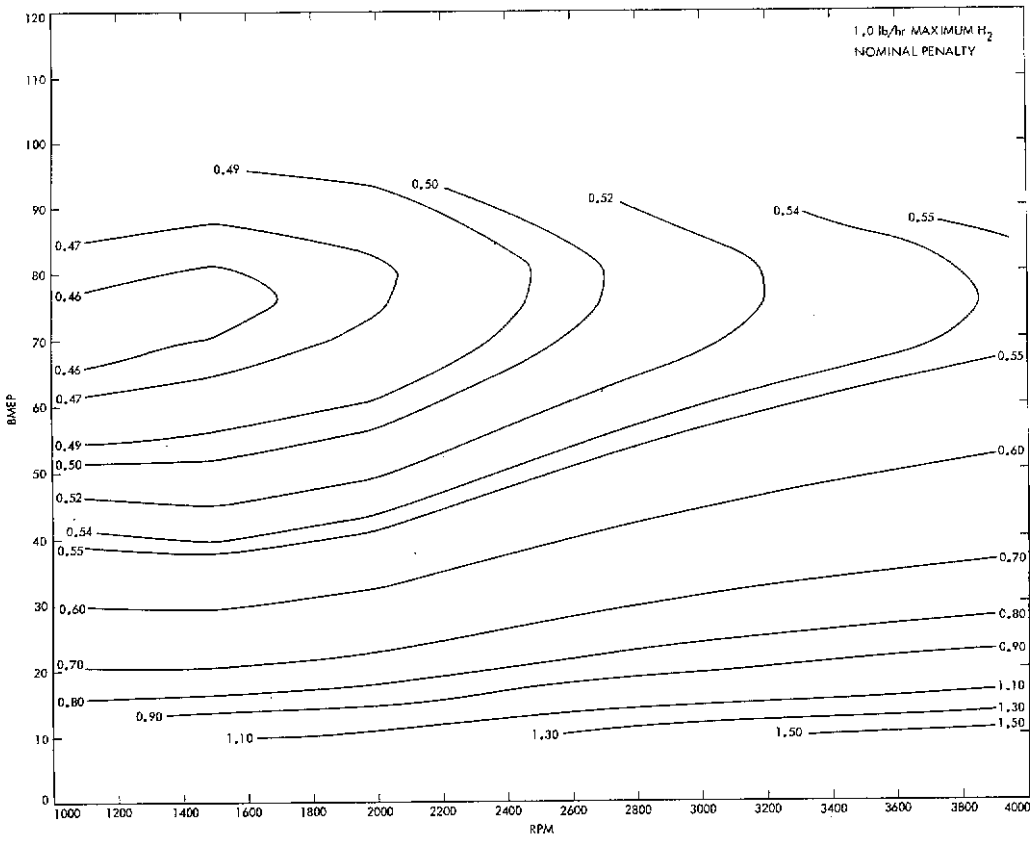

Fig. 13 - BSFC contour plot with controlled H_2 flow

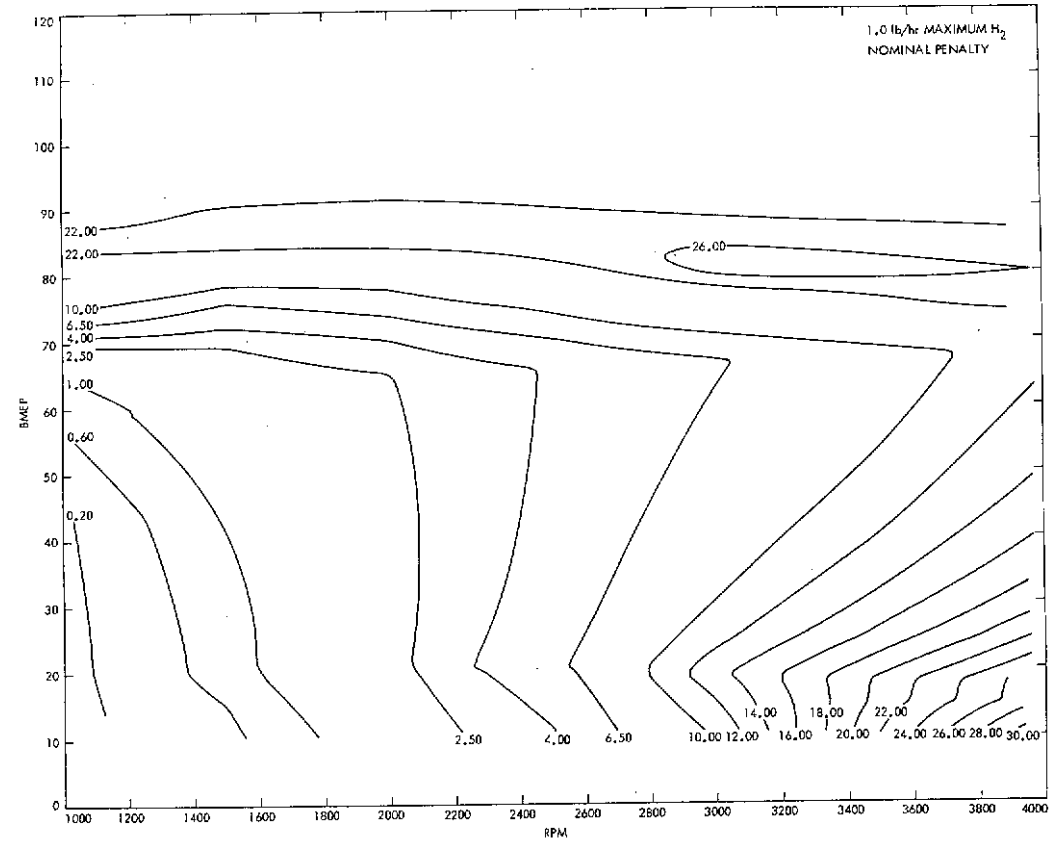

Fig. 14 - $BSNO_X$ contour plot with controlled H_2 flow

the Federal Driving Cycle (FDC), (10) a simulation of this driving cycle was developed. In this simulation the FDC was broken up into 1-second increments, and for each increment the required engine brake horsepower output and engine speed were calculated. The output of the system model was then used to provide an estimate of the fuel consumption and NO_x production in this increment. The contributions of all the increments were then aggregated and the results presented as fuel consumption in mile/gallon and NO_x emissions in gm/mile.

Because the predictions of the system model were for steady-state operation at each operating point, it was expected that the estimated mileage and NO_x emissions would be optimistic. That is, the neglect of transient demands and responses would provide estimates of mileage and emissions better than the actual data.

To obtain the estimates presented herein, the vehicle characteristics used in the FDC simulation were those of a 1973 Chevrolet Impala, an inertia wheel simulating a 4500 lbm vehicle, with an automatic transmission (three-speed Turbo-Hydramatic transmission), and a 2.73:1 differential (See Fig. 15).

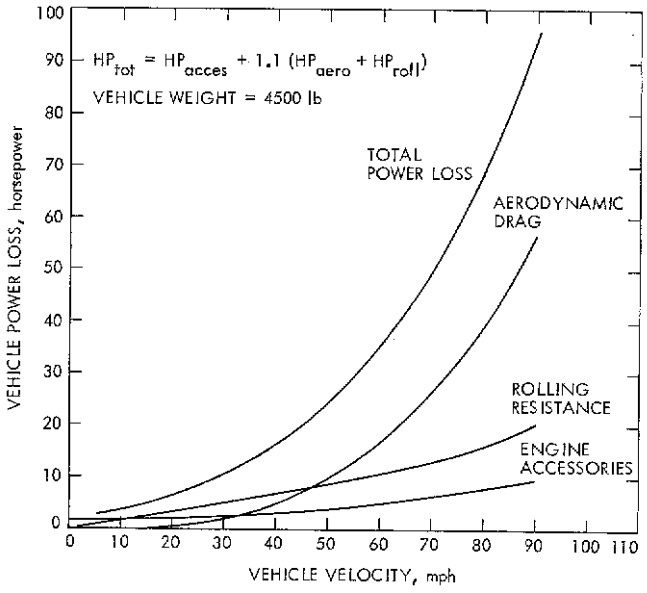

Fig. 15 - Vehicle power consumption characteristics for FDC simulation

To assess the quality of this simulation, two check cases were run in which the FDC simulation using engine dynamometer data as input was compared to the data obtained actually running similarly equipped vehicles through the driving cycle on a chassis dynamometer. The two check cases consisted of:

(1) The stock 1973 Chevrolet Impala vehicle, with all factory-installed emissions equipment, and engine dynamometer data taken from a similar, stock 1973 350 CID Chevrolet V-8.

(2) A similar vehicle and engine but with the induction and ignition systems replaced by the Electrosonic III induction and ignition systems (Autotronics Controls Corp., El Paso, Texas). Both the vehicle and engine were operated at an equivalence ratio, neglecting enrichments, of 0.85 with gasoline. Except for the PCV system none of the emissions control equipment was operating.

Table 3 presents a comparison of the fuel consumption and emissions measured with the vehicle and that predicted by the FDC simulation using steady-state engine dynamometer data. It can be seen that the predicted fuel consumption is approximately 14% better than the measured stock fuel consumption (on a mpg basis), and that of the modified vehicle was 8% better. The predicted NO_x emissions were within 8% of the measured values in both cases.

Table 3. Predicted and Measured Results for Federal Urban Driving Cycle with 1973 Chevrolet Impala V-8 (350 CID Stock Engine)

	Driving Cycle Results			
	Measured (chassis dynamometer)		Predicted (using engine dynamometer data)	
Carburetor Configuration	Fuel Economy (mpg)	NO_x Emissions (gm/mi)	Fuel Economy (mpg)	NO_x Emissions (gm/mi)
Stock	10.6	2.05	12.11	2.16
Autotronics*	12.8	5.12	13.82	5.54

The FDC simulation program was used to estimate the performance of a 1973 Chevrolet Impala vehicle using a hydrogen generator/engine system. The BSFC and $BSNO_x$ of this system were predicted using the system model. The cases for which predictions were made are summarized in Table 4. Estimates made for the 8.5:1 compression ratio (CR), current lean limit, and no auxiliary hydrogen generator subsystem loads correspond to the cases for which comparison to engine dynamometer data was made above. For the same engine configuration, the effect of adding the

Table 4. Engine/Hydrogen Generator Cases Studied

Engine Configuration		Auxiliary Loss			
CR	LL	None	Minimum	Nominal	Maximum
8.5	Current	x	x	x	x
8.5	50%			x	
8.5	75%			x	
10.0	75%	x		x	

CR = compression ratio; LL = lean limit.

*All emission equipment except PCV disconnected

hydrogen generator subsystem auxiliary loads was assessed for each of the three load conditions: minimum, nominal, and maximum.

Table 5 presents these data. The estimates should be carefully distinguished from those presented in Table 3. Table 3 presents a comparison of estimates of fuel consumption and NO_X emissions made by a FDC simulation program using steady-state engine dynamometer data with actual FDC measurements obtained using similar engines in 1973 Impala vehicles. Tables 5 and 6 present estimates of the performance of hydrogen-supplemented fuels systems. These estimates were made using BSFC and $BSNO_X$ predictions made with the system model as inputs to the FDC simulation program. The fuel consumption estimates were also indexed back to the estimated stock fuel consumption, 12.11 mpg.

In Table 5 the effects of the auxiliary loads from the hydrogen generator subsystem are seen to decrease mileage less than 4% and to increase NO_X emission less than 18%, both small effects. The remainder of the predictions were therefore made only for the nominal hydrogen generator subsystem auxiliary loads.

Table 5. Predicted Fuel Economy and NO_X Emissions for Federal Urban Driving Cycle with Theoretical Engine Performance

Configuration		Hydrogen	Fuel Economy		NO_X
Engine	Generator System	Flow (lbm/hr)	MPG	Improvement (%)	Emissions (gm/mi)
Baseline	No penalty	0.5	14.69	21.3	1.30
		1.0	14.99	23.8	0.86
		Controlled	14.76	21.9	0.43
Baseline	Minimum penalty	0.5	14.47	19.5	1.38
		1.0	14.60	20.6	0.97
		Controlled	14.43	19.2	0.50
Baseline	Nominal penalty	0.5	14.41	19.0	1.38
		1.0	14.58	20.4	0.98
		Controlled	14.42	19.1	0.50
Baseline	Maximum penalty	0.5	14.25	17.7	1.38
		1.0	14.52	19.9	1.00
		Controlled	14.40	18.9	0.51

The effect of assuming the engine lean operating limit could be improved to the 50 and 75% improved lean limits was assessed as was the effect of increasing compression ratio to 10:1 from the stock 8.5:1. The results of these calculations are presented in Table 6. For convenience, the fuel consumption data are presented both as predicted miles/gallon and as the percent improvement over the predicted stock carburetted engine performance, 12.11 mpg. Because the comparison of the NO_X emissions with the engine dynamometer data indicated that the model tended to overestimate NO_X production, it was felt that the predicted emissions were not unrealistic.

Table 6. Predicted Fuel Economy and NO_X Emissions for Federal Urban Driving Cycle with Theoretical Engine Performance

Configuration		Hydrogen	Fuel Economy		NO_X
Engine	Generator System	Flow (lbm/hr)	MPG	Improvement (%)	Emissions (gm/mi)
Baseline	Nominal penalty	0.5	14.41	19.0	1.38
		1.0	14.58	20.4	0.98
		Controlled	14.42	19.1	0.50
Lean Limit improved 50%	Nominal penalty	0.5	14.91	23.1	0.27
		1.0	14.85	22.6	0.85
		Controlled	14.69	21.3	0.27
Lean limit improved 75%	Nominal penalty	0.5	15.07	24.4	0.29
		1.0	14.93	23.3	0.86
		Controlled	14.90	23.0	0.29
Compression ratio = 10:0:1 Lean limit improved 75%	Nominal penalty	0.5	15.47	27.7	0.20
		1.0	15.41	27.3	0.70
		Controlled	15.26	26.0	0.20

It can be seen from Table 6 that improving the ability of the engine to operate at a lean condition (to the 50% improved lean limit constraint) is predicted to result in a 20% improvement in fuel economy and produce NO_X emissions less than 0.4 gm/mile. Improving the lean limit to the 75% improved lean limit is predicted to result in a 23% improvement in fuel economy with NO_X emissions less than 0.2 gm/mile. Increasing compression ratio to 10:1 again with operation at the 75% improved lean limit constraint is predicted to result in 25% improved fuel economy and NO_X emissions of about 0.2 gm/mile.

HC AND CO EMISSIONS

The emissions of unburned hydrocarbons and carbon monoxide have not been dealt with in these analyses. This is because it has not been possible, to date, to develop and incorporate an adequate model of the production of these pollutants. However, in any combustion concept relying on lean operation, these emissions have proven troublesome because the resulting reduction in combustion temperature yields higher emission levels and impairs the effective use of an oxidizing catalyst. To determine if a catalyst would operate with a hydrogen-supplemented fuels system, a 1975 Chevrolet Impala converter was added to the bottled hydrogen vehicle. (1)

Table 7 presents a comparison of the energy consumption and emissions of this vehicle in the stock, hydrogen-enriched, and hydrogen-enriched-with-converter configurations. The significant reduction in both HC and CO emissions yields confidence that upcoming tests using this converter with a hydrogen generator/engine system will yield similar improvements in these emissions.

These data are the result of work described in a paper submitted for presentation at the 10th IECEC Conference (1975).

Table 7. Effect of Catalytic Muffler on Emissions of Hydrogen-Enriched Vehicle Over Federal Driving Cycle

Parameter	Stock	Hydrogen Enriched: Without Catalytic Muffler	Hydrogen Enriched: With Catalytic Muffler
NO_X (gm/mi)	1.75	0.31	0.28
CO (gm/mi)	43.91	2.22	0.07
HC (gm/mi)	2.29	3.11	0.45
Fuel consumption (Btu/mi)	12,700	8,850	8,850

CONCLUSIONS

Analytical models of the hydrogen-enriched fuels system have permitted an estimate of the potential of this system to be made. These models consisted of representations of a hydrogen generator subsystem, a system comprised of a V-8 engine and this subsystem, and a simulation of the Federal Driving Cycle. Results of applying these analyses to a 350 CID Chevrolet engine and a 1973 Chevrolet Impala vehicle were presented in Tables 5 and 6.

Comparison of the predictions of these models and simulations with data taken on the engine dynamometer and chassis dynamometer indicated satisfactory agreement between the data and the predictions.

An assessment of the effect of improving the engine lean operating constraint and of increasing engine compression ratio from 8.5:1 to 10:1 indicated that a 25% improvement in fuel economy over the Federal Driving Cycle (relative to the unmodified vehicle) would result and NO_X production would be reduced to 0.2 gm/mile.

Emissions of carbon monoxide and unburned hydrocarbons were not modeled. Data taken on the bottled gas car using a 1975 Chevrolet Impala catalytic exhaust converter indicated that significant reductions in these emissions should be observed in upcoming tests with such a converter on a hydrogen generator/engine system.

REFERENCES

1. F. W. Hoehn and M. W. Dowdy, "Feasibility Demonstration of a Road Vehicle Fueled with Hydrogen-Enriched Gasoline," IECEC Paper 749105, 1974.

2. Kurt H. Weil, "The Hydrogen IC Engine - Its Origins and Future in the Emerging Energy - Transportation - Environment Systems," SAE Paper 729212, 1972.

3. J. Houseman and D. J. Cerini, "On-Board Hydrogen Generator for a Partial Hydrogen Injection Internal Combustion Engine," SAE Paper 740600, 1974.

4. J. Houseman and F. W. Hoehn, "A Two-Charge Engine Concept: Hydrogen Enrichment," SAE Paper 741169, 1974.

5. "ASHRAE Guide and Data Book - Systems and Equipment," American Society of Heating, Refrigerating and Air Conditioning Engineers, 1967.

6. N. F. Pederson, "The Statistical and Analytical Approach to Determining Pump Performance," presented at Aerospace Fluid Power Conference, Detroit, Michigan, Oct. 28-29, 1963.

7. H. F. Coward and G. W. Jones, "Limits of Flammability of Gases and Vapors," Bull. 503, Bureau of Mines, U. S. Department of Interior, pp. 6-18, 118, 1952.

8. Final Report, "Engine/Generator Performance Maps," performed for Environmental Protection Agency under NASA OAST Resources-Authority-Warrant Serial No. 53/74R, Task Order RD-152 (to be published).

9. P. Blumberg and J. T. Kummer, "Prediction of NO Formation in Spark-Ignited Engines - An Analysis of Methods of Control," Combustion Science and Technology, Vol. 4, pp. 73-95, 1971.

10. Federal Register, Vol. 37, No. 221, Nov. 15, 1972.

APPENDIX

RELATIONSHIPS OF ENGINE SPEED, EQUIVALENCE RATIO, THROTTLE SETTING, ENGINE/HYDROGEN GENERATOR FLOW RATES, AND EFFECTIVE EQUIVALENCE RATIO

CALCULATION OF VOLUME FLOW CONSTRAINT

Equivalence ratio of the engine, ϕ_E:

$$\phi_E = \frac{\text{stoichiometric air flow rate based on flow rate of gasoline to the engine} + \text{stoichiometric air flow rate based on flow rate of hydrogen generator products to the engine}}{\text{actual flow rate of air to the engine}}$$

Let ζ_i be the stoichiometric fuel/air ratio for the i^{th} fuel; then

$$\phi_E = \frac{\frac{\dot{m}_{gE}}{\zeta_g} + \frac{\dot{m}_G}{\zeta_{pG}}}{\dot{m}_{aE}}$$

where $\dot{m}_i$ is the mass flow rate of the i^{th} component; subscripts g, a, p, and G refer to gasoline, air, generator products, and hydrogen generator total flowrate

respectively; and subscripts E and G refer to engine and hydrogen generator respectively.

If we let ϕ_G be the equivalence ratio of the hydrogen generator input gasoline and air (typically its value is 2.75), we can write

$$\frac{\dot{m}_G}{\zeta_{pG}} = \frac{\dot{m}_{gG}}{\zeta_g}\left(1 - \frac{1}{\phi_G}\right)$$

and then

$$\phi_E = \frac{\frac{\dot{m}_{gE}}{\zeta_g} + \frac{\dot{m}_{gG}}{\zeta_g}\left(1 - \frac{1}{\phi_G}\right)}{\dot{m}_{aE}}$$

Normalizing with respect to $\dot{m}_G$ yields

$$\phi_E = \frac{\frac{1}{\zeta_g}\frac{\psi}{\left(1 + \frac{1}{\zeta_g\phi_G}\right)} + \frac{\zeta_g\phi_G}{1 + \zeta_g\phi_G}\left(1 - \frac{1}{\phi_G}\right)}{\frac{\dot{m}_{aE}}{\dot{m}_G}}$$

where

$$\psi = \frac{\dot{m}_{gE}}{\dot{m}_{gG}}$$

Solving for ψ we obtain

$$\psi = \zeta_g\left[\phi_E\frac{\dot{m}_{aE}}{\dot{m}_G} - \frac{\zeta_g\phi_G}{1 + \zeta_g\phi_G}\left(1 - \frac{1}{\phi_G}\right)\right]\left(1 + \frac{1}{\zeta_g\phi_G}\right)$$

The total volume flow through the engine at any throttle setting is

$$\dot{V} = \tau e_v \frac{N}{2} V_D$$

where

τ = throttle setting
e_v = wide open throttle volumetric efficiency
N = engine rotation rate
V_D = engine displacement = $\pi/4$ (bore)^2 (stroke) (number of cylinders)

However,

$$\dot{V} = \frac{\dot{m}_{aE}}{\rho_a} + \frac{\dot{m}_G}{\rho_{pG}}$$

where

ρ_i = mass density of i^{th} component

and

$\dot{m}_G$ = total hydrogen generator mass flow rate

Assuming that the temperature of the air and of the generator products are the same when mixed in the engine,

$$\dot{V} = \frac{\dot{m}_G}{\rho_{pG}}\left(\frac{\dot{m}_{aE}}{\dot{m}_G}\frac{\bar{m}_{pG}}{\bar{m}_a} + 1\right)$$

where

$\bar{m}_i$ is the molecular weight of the i^{th} component

Then

$$\frac{\dot{m}_{aE}}{\dot{m}_G} = \left(\frac{\tau e_v \frac{N}{2} V_D \rho_{pG}}{\dot{m}_G} - 1\right)\frac{\bar{m}_a}{\bar{m}_{pG}}$$

Since the hydrogen generator total flow rate is proportional to hydrogen flow rate,

$$\dot{m}_H = K_H \dot{m}_G$$

where m_H is the hydrogen mass flow rate

$$\frac{\dot{m}_{aE}}{\dot{m}_G} = \left(\frac{\tau e_v \frac{N}{2} V_D \rho_{pG} K_H}{\dot{m}_H} - 1\right)\frac{\bar{m}_a}{\bar{m}_{pG}}$$

and substituting into the previously derived expression for ψ we obtain

$$\psi = \zeta_g\left[\left(\frac{\tau e_v \frac{N}{2} V_D \rho_{pG} K_H}{\dot{m}_H} - 1\right)\frac{\bar{m}_a}{\bar{m}_{pG}}\phi_E - \frac{\phi_G}{1 + \zeta_g\phi_G}\left(1 - \frac{1}{\phi_G}\right)\right]\left(1 + \frac{1}{\zeta_g\phi_G}\right) \quad \text{(A-1)}$$

CALCULATION OF EFFECTIVE EQUIVALENCE RATIO

Define effective equivalence ratio ϕ'_E as

$$\phi'_E = \frac{\begin{array}{l}\text{stoichiometric air flow rate based on flow rate of gasoline to the engine}\end{array}}{\begin{array}{l}\text{actual flow rate of air to the engine}\end{array}} + \frac{\begin{array}{l}\text{stoichiometric air flow rate based on flow rate of hydrogen generator products to the engine}\end{array}}{\begin{array}{l}\text{actual flow rate of noncombustibles to the engine}\end{array}}$$

The flow rate of noncombustibles to the engine $\dot{m}_{DIL}$ provided by the hydrogen generator is

$$\dot{m}_{DIL} = \dot{m}_G - \dot{m}_H + \dot{m}_{CO} + \dot{m}_{CH_4}$$

where subscripts DIL, G, H, CO, CH_4 refer to diluent, hydrogen generator, hydrogen carbon monoxide, and methane, respectively, and

$$\dot{m}_{DIL} = \dot{m}_G \left(1 - K_H + K_{CO} + K_{CH_4}\right)$$

where K_i is the mass fraction of the i^{th} constituent in the hydrogen generator product stream.

Then

$$\phi'_E = \frac{\dfrac{\dot{m}_{gE}}{\zeta_g} + \dfrac{\dot{m}_G}{\zeta_g} \dfrac{1 - \dfrac{1}{\phi_G}}{1 + \dfrac{1}{\zeta_g \phi_G}}}{\dot{m}_{aE} + \dot{m}_G \left(1 - K_H + K_{CO} + K_{CH_4}\right)}$$

Normalizing as before we obtain

$$\phi'_E = \frac{\dfrac{1}{\zeta_G}\left[\dfrac{\psi}{\left(1 + \dfrac{1}{\zeta_g \phi_G}\right)} \dfrac{\zeta_g \phi_G}{1 + \zeta_g \phi_G}\left(1 - \dfrac{1}{\phi_G}\right)\right]}{\dfrac{\dot{m}_{aE}}{\dot{m}_G} + 1 - \left(K_H + K_{CO} + K_{CH_4}\right)}$$

Since

$$\phi_E = \frac{\dfrac{1}{\zeta_G}\left[\dfrac{\psi}{\left(1 + \dfrac{1}{\zeta_g \phi_G}\right)} + \dfrac{\zeta_g \phi_G}{1 + \zeta_g \phi_G}\left(1 - \dfrac{1}{\phi_G}\right)\right]}{\dfrac{\dot{m}_{aE}}{\dot{m}_G}}$$

Then

$$\phi'_E = \frac{\dfrac{1}{\zeta_g}\left[\dfrac{\psi}{\left(1 + \dfrac{1}{\zeta_g \phi_G}\right)} + \dfrac{\zeta \phi}{1 + \zeta_g \phi_G}\left(1 - \dfrac{1}{\phi_G}\right)\right]}{\dfrac{1}{\zeta_g \phi_E}\left[\psi\left(1 + \dfrac{1}{\zeta_g \phi_G}\right) + \dfrac{\zeta_g \phi_G}{1 + \zeta_g \phi_G}\left(1 - \dfrac{1}{\phi_E}\right) + 1 - \left(K_H + K_{CO} + K_{CH_4}\right)\right]} \quad \text{(A-2)}$$

Equations (A-1) and (A-2) represent a set of relations between which the engine volume flow constraint is a function only of ψ and ϕ'_E.

Society of Automotive Engineers, Inc.
400 COMMONWEALTH DRIVE, WARRENDALE, PA. 15096

16 page booklet.

Printed in U.S.A.